$$\vec{H}(r,t) = -\frac{I_0 l \sin\theta}{4\pi r^2}\hat{\phi}$$

Since the Poynting vector $\vec{S}(\vec{r},t) = \left(\vec{E}(\vec{r},t) \times \vec{H}^*(\vec{r},t)\right)$ is imaginary and negative, near fields correspond to a reactive power and a stored electric energy.

The equivalent Thévenin impedance $Z_A(\omega)$ of the antenna is expressed by:

$$Z_A(\omega) = R_A(\omega) + jX_A(\omega)$$

$R_A(\omega)$ is the resistive part of the impedance corresponding to the total radiated power.

$X_A(\omega)$ is the reactive part corresponding to the energy stored in the near field.

3.6. Characteristics of networks of microwave antennas

The microwave domain covers the range of frequencies between 300 MHz and 300 GHz. The main applications of the networks of microwave antennas are radar systems and the fifth generation (5G) of mobile telecommunication systems.

3.6.1. *Introduction to networks of microwave antennas*

Radar systems use microwave antennas to detect targets. A detection sequence involves microwave radiation emission by the antenna, then reception and analysis of the waves re-emitted by the target.

Radar systems technology went through several development stages. The systems were initially built with parabolic antennas, which were moved mechanically [SIL 49]. Consequently, the use of networks of passive antennas with phase retardation made it possible to control the emission beam direction and to improve the scanning sensitivity of the beam. Due to the network configuration of antennas, emitted waves interfered

constructively in the desired target directions and destructively in the complementary space, which lead to an increased directivity of the antenna. The use of drive electronics to control the phase retardation of each antenna of the network made it possible to define the emission/reception beam direction. These systems had no moveable mechanical parts. As the emission and reception electronic modules were often integrated near the antenna network, the maintenance of these radar systems was simplified and their reliability improved. Finally, radar systems were developed around active antenna networks with phase retardation. The presence of an amplifier circuit and a phase adjustment circuit at each antenna of the network enables the numerical control of the emitted or received beam.

Compared to the previous generations (2G, 3G, 4G) of mobile telephony systems, the fifth generation (5G) is a breakthrough technology. 5G telecommunication systems can direct the radiated energy at very high frequency towards the users. They offer very high data transfer rates and very short delays for data transit. They can simultaneously connect to the Internet network a large number of objects. Being compact, they can be installed on the fourth generation equipment towers (Figure 3.7). The frequency bands of the fifth generation (5G) mobile telephony systems are at the present time: 3.3–3.8 GHz and 6–10 GHz.

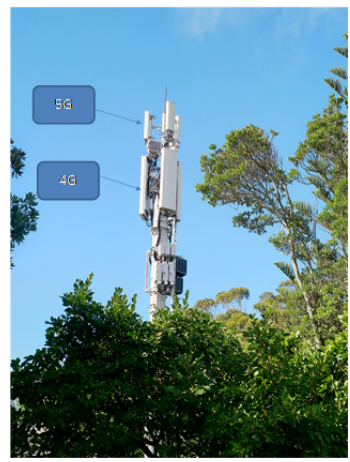

Figure 3.7. *Block of four 5G antennas operating at 3.5 GHz installed above 4G antennas. For a color version of this figure, see www.iste.co.uk/dahoo/metrology1.zip*

5G antennas are made of networks of antennas in which individual antennas are separated by about one-half wavelength. The addition of a phase retardation to the signal transmitted or received by each antenna enhances the properties of the collective signal of the network of antennas compared to those of individual antennas. The power radiated by the network is higher than that of an isolated antenna. The beam is narrower. It is possible to direct the emission/reception beam at the phase retardation control frequency.

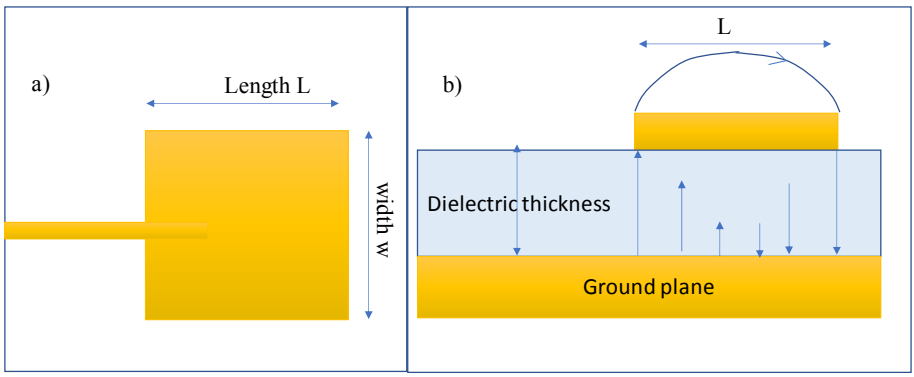

Figure 3.8. *Schematic diagram of a patch antenna: a) top view of the rectangle conductor whose length L is about λ/2 and b) sectional view of the resonant cavity and radiated electric field (blue). For a color version of this figure, see www.iste.co.uk/dahoo/metrology1.zip*

5G antennas are often constituted of networks of patch antennas (Figure 3.8). Patch antennas are planar radiative structures. They can, for example, be obtained by etching on a printed circuit. They are formed of a metallic layer of rectangular, circular or arbitrary geometry, deposited on the dielectric layer of a printed circuit. The opposite face of the printed circuit is metallic and operates as a ground plane. The patch, the ground plane and the four edges form a cavity that can be excited by a microwave of wavelength λ. The length of the patch is of the order of λ/2. The thicknesses of the conducting and dielectric layers are often very small compared to the wavelength. When the patch is supplied by a microstrip line, it enters into resonance, similarly to a half-wave dipole. Excitation generates in phase diffracted electric fields on the edges of the antenna. Due to the ground plane, radiation occurs only in the half-plane above the ground plane. If each antenna has a phase shift circuit and a minimizing circuit, the delay and the

amplitude of the current of each antenna in the network can be numerically controlled. The use of numerical control techniques makes it possible to form a beam and move this beam at a very high frequency. Several beams can be emitted simultaneously by a network of antennas. This provides a good signal to noise ratio and improves data transfer rate.

3.6.2. *Radiation of antenna networks*

To illustrate the operating principle of a network antenna with phase retardation, let us consider a network of N equidistant antennas separated by a distance D, supplied by a current of periodic amplitude $I = \frac{I_0}{\sqrt{N}}\cos(\omega t - \varphi_N)$ (see Figure 3.9).

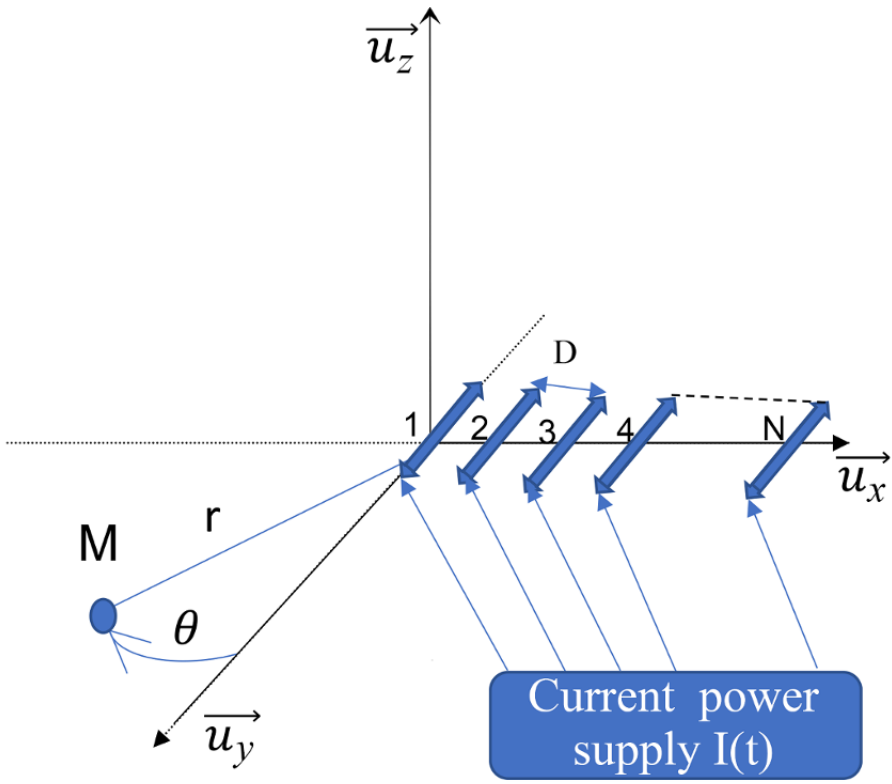

Figure 3.9. *Network of N current-supplied antennas. For a color version of this figure, see www.iste.co.uk/dahoo/metrology1.zip*

The purpose is to study the total electric field radiated at infinity. The antennas are directed along $\overrightarrow{u_y}$. They are lined up along $\overrightarrow{u_x}$ and the field in plane ($\overrightarrow{u_z}, \overrightarrow{u_y}$) is studied along a direction given by θ:

1) Assume that $\varphi_N = 0$, for all N. For a point M, at a distance r from the network, with r $\gg ND$, write the delay as a function of I, D,θ c. Calculate E_i^* as a function of E_1^*. Then, deduce the sum of the amplitudes $E(\theta)$. Draw the radiation diagram $|E^*(\theta)|^2$ as a function of θ for a network of eight antennas spaced at a distance $D = \lambda$ for a wavelength λ of 0.03 m in the limit $\left(\frac{D}{\lambda}\right) sin\theta \ll 1$.

2) Delays of $0, \tau, 2\tau, 3\tau, \ldots, (N-1)$ are introduced on the supply line 1,2,3,..,N, respectively (Figure 3.10). What does this mean for the phases φ_N? As $(\varphi_{i-1} - \varphi_i) \leq 2\pi$, deduce the useful range of delays τ. Then, calculate $E_\tau(\theta)$ and $E_\tau^2(\theta)$.

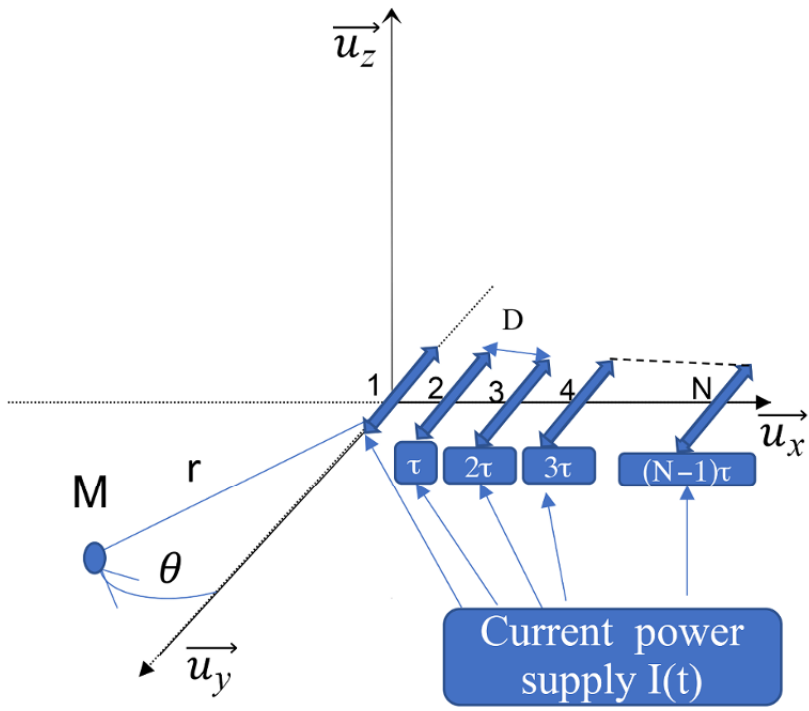

Figure 3.10. *Delays applied to the N antennas of the network. For a color version of this figure, see www.iste.co.uk/dahoo/metrology1.zip*

Draw the new radiation diagram for a delay $\tau = 4.10^{-11}(s)$.

Why is this referred to as beam steering?

3) How does the diagram change if, in addition, the delay system introduces an attenuation a = (1-ε)? Draw the new radiation diagram for a coefficient of attenuation a = (1-ε) = 0.95 and a delay $\tau = 4.10^{-11}(s)$.

4) Draw an analogy of the configuration at question 1) to the light wave falling on an etched plate with each roughness being considered as an individual reflector, at normal incidence. Do the same for the configuration at question 2) at oblique incidence θ_i. Find the relation between θ_i and τ. Finally, consider the case in the limit $D\frac{sin\theta}{l} > 1$.

3.6.2.1. *Answer to question 1*

Each antenna i of the network emits an electric field $\vec{E}_i$ given by:

$$\vec{E}_i = \frac{A}{r_i}\cos\left(\omega(t-\frac{r_i}{c})+\varphi_i\right)\overrightarrow{u_y}$$

For a point M in the plane ($\overrightarrow{u_x}, \overrightarrow{u_y}$), the amplitude of the electric field $\vec{E}_i$ of the ith antenna of the network is given by:

$$E_i = j\frac{l}{2\lambda}\frac{sin\theta}{r_i}\sqrt{\frac{\mu_0}{\nu_0}}\frac{I_0}{\sqrt{N}} = \frac{A}{r_i}$$

If the observation point of the radiated field is far from the antenna network, then:

$$\frac{A}{r_i} \approx \frac{A}{r}$$

where r designates the distance from antenna 1 of the network to the point M, and $r \gg ND$.

The electric field radiated by each antenna is: $E_{ref} = j\frac{l}{2\lambda}\frac{sin\theta}{r}\sqrt{\frac{\mu_0}{\nu_0}}\frac{I_0}{\sqrt{N}}$.

Since vectors $\vec{r_i}$ are parallel (see Figure 3.11):

$$r_2 = r_1 - Dsin\theta$$

By recurrence: $r_i = r_1 - (i-1)Dsin\theta$

and: $\frac{r_i}{c} = \frac{r_1}{c} - (i-1)\frac{D}{c}sin\theta$

To obtain the contribution $\sum_{i=1}^{N} \vec{E_i}$ of all the antennas in the network, the harmonic expression $\overrightarrow{E_i^*}$ of the electric field parallel to $\overrightarrow{u_y}$ radiated by the ith antenna is used.

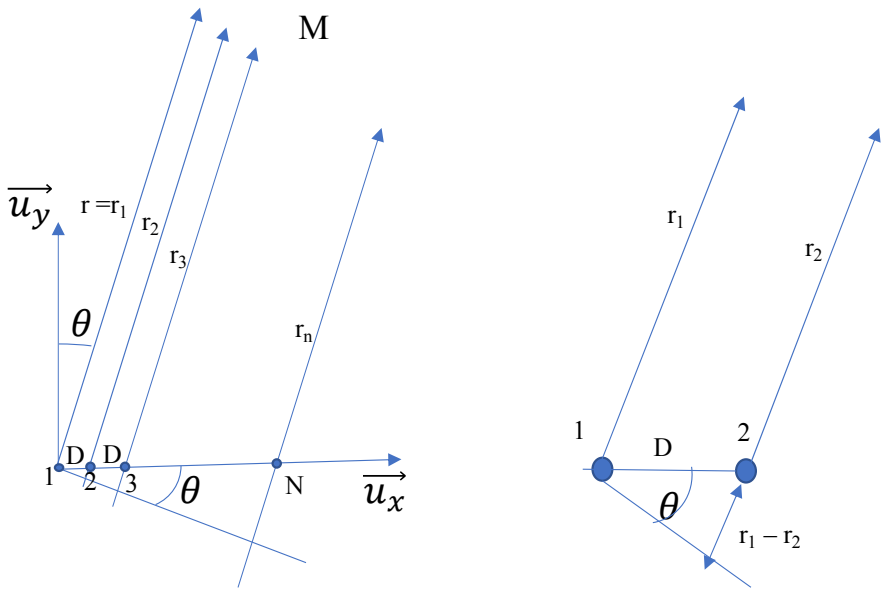

Figure 3.11. *Applied delay. For a color version of this figure, see www.iste.co.uk/dahoo/metrology1.zip*

Let E_i^* be the component y of the radiated electric field:

$$E_i^* = E_{ref} \exp(j\omega\left(t - \frac{r_i}{c}\right) + \varphi_i)$$

As $\varphi_i = 0$,

$$E_i^* = E_{ref} \exp(j\omega \left(t - \frac{r_1}{c} - \frac{(i-1)D}{c} sin\theta \right)$$

$$E_i^* = E_{ref} \exp(j \left(\omega(t - \frac{r_1}{c}) - (i-1) \left(\frac{\omega D}{c} sin\theta\right)\right)$$

Since $\frac{\omega D}{c} = \frac{2\pi \nu D}{c} = \frac{2\pi D}{\lambda}$

$$E_i^* = E_1^* \exp \left(-2\pi j(i-1)(\frac{\omega D}{c} sin\theta) \right)$$

$$= E_1^* \exp \left(-2\pi j(i-1)(\frac{D}{\lambda}) sin\theta \right)$$

The field radiated by the network is expressed as:

$$\sum_{i=1}^{N} E_i^* = E_1^* \sum_{i=1}^{N} \exp \left(-2\pi j(i-1)(\frac{D}{\lambda}) sin\theta \right)$$

$$= E_1^* \sum_{i'=0}^{N-1} \exp \left(-2\pi j(i')(\frac{D}{\lambda}) sin\theta \right)$$

$\sum_{i=1}^{N} E_i^*$ is a geometric series that can be easily summed using the formula: $1+a+\ldots+a^{N-1} = \frac{1-a^N}{1-a}$

$$\sum_{i=1}^{N} E_i^* =$$

$$E_1^* \frac{1-\exp(-2\pi jN\left(\frac{D}{\lambda}\right) sin\theta)}{1-\exp(-2\pi j\left(\frac{D}{\lambda}\right) sin\theta)} =$$

$$E_1^* \frac{\exp\left(-j\pi N\left(\frac{D}{\lambda}\right)\right)}{\exp\left(-j\pi\left(\frac{D}{\lambda}\right)\right)} \frac{\exp(j\pi N\left(\frac{D}{\lambda}\right) sin\theta) - \exp(-j\pi N\left(\frac{D}{\lambda}\right) sin\theta)}{\exp(j\pi\left(\frac{D}{\lambda}\right) sin\theta) - \exp(-j\pi\left(\frac{D}{\lambda}\right) sin\theta)}$$

$$\sum_{i=1}^{N} E_i^* = E_1^* e^{-(j\pi(N-1)\frac{D}{\lambda})} \frac{\sin(\pi N\left(\frac{D}{\lambda}\right) sin\theta)}{\sin(\pi\left(\frac{D}{\lambda}\right) sin\theta)}$$

$$E(\theta)^2 = E_{ref}^2 \frac{sin^2(\pi N \left(\frac{D}{\lambda}\right) sin\theta)}{sin^2(\pi \left(\frac{D}{\lambda}\right) sin\theta)}$$

If θ is small and N is large or more precisely if $\left(\frac{D}{\lambda}\right) sin\theta \ll 1$ or still if $sin\theta \ll \frac{\lambda}{D}$, then:

$$E(\theta)^2 = E_{ref}^2 \frac{sin^2(\pi N\left(\frac{D}{\lambda}\right)sin\theta)}{sin^2(\pi\left(\frac{D}{\lambda}\right)sin\theta)} = \left(\frac{l}{2\lambda}\frac{sin\theta}{r}\right)^2 \sqrt{\frac{\mu_0}{\varepsilon_0}} \frac{I_0^2}{N} \frac{sin^2(\pi N\left(\frac{D}{\lambda}\right)sin\theta)}{(\pi N\left(\frac{D}{\lambda}\right)sin\theta)^2}$$

$$E(\theta)^2 = \left(\frac{l}{2\lambda}\frac{sin\theta}{r}\right)^2 \sqrt{\frac{\mu_0}{\varepsilon_0}} \frac{I_0^2}{N} sinc^2(\pi N \left(\frac{D}{\lambda}\right) sin\theta)$$

The first zero is obtained when $N\frac{D}{\lambda} sin\theta = 1$.

Let us consider: $sin\theta = \frac{\lambda}{ND}$

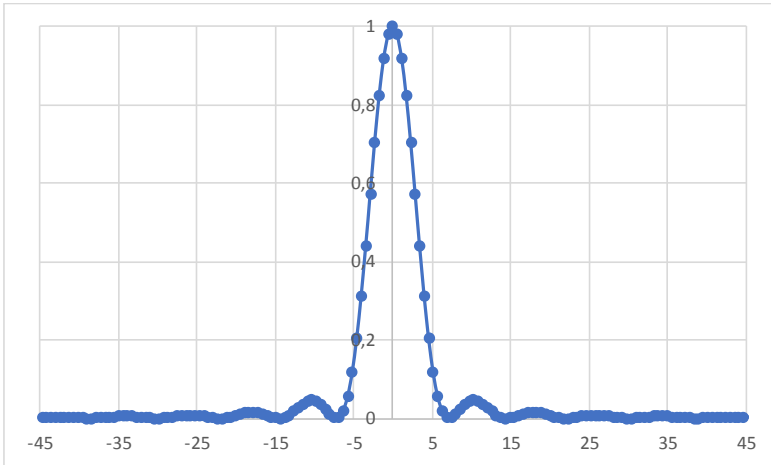

Figure 3.12. *Radiation diagram $E(\theta)^2$ of a network of eight antennas as a function of the angle θ (degrees) for $\frac{D}{\lambda} = 1$. For a color version of this figure, see www.iste.co.uk/dahoo/metrology1.zip*

Figure 3.12 shows the radiation diagram $|E^*(\theta)|^2$ as a function of θ of a network of eight antennas spaced at a distance $D = \lambda$ for a wavelength λ of 0.03 m.

The width of the main peak is: $2\frac{\lambda}{ND} \sim \frac{2}{N}$ if $\lambda \sim D$.

3.6.2.2. *Answer to question 2*

When there are delays on each antenna of the network, it can be noted that the delay φ_i of the antenna i is expressed by:

$$\varphi_i = \omega\tau_i = \omega(i-1)\tau$$

Such that:

$$\omega(t - \tau_{i)} = \omega t - \omega(i-1)\tau$$

Hence:

$$E_i^* = E_1^* \exp\left(-j(i-1)\frac{2\pi}{\lambda}(Dsin\theta - \tau\nu)\right)$$

As $\nu = \frac{c}{\lambda}$, τ is significant if $2\pi\tau\nu \leq 2\pi$

$$E_i^* = E_1^* \exp\left(-j(i-1)\frac{2\pi D}{\lambda}\left(sin\theta - \tau\frac{\nu}{D}\right)\right), \text{ and:}$$

$$E_i^* = E_1^* \exp\left(-j(i-1)\frac{2\pi D}{\lambda}\left(sin\theta - \tau\frac{c}{D}\right)\right)$$

$$\sum_{i=1}^{N} E_i^* = E_1^* e^{-(j\pi(N-1)\frac{D}{\lambda})} \frac{\sin(\pi N\left(\frac{D}{\lambda}\right)\left(sin\theta - \tau\left(\frac{c}{D}\right)\right))}{\sin(\pi\left(\frac{D}{\lambda}\right)\left(sin\theta - \tau\left(\frac{c}{D}\right)\right))}$$

$$E(\theta)^2 = E_{ref}^2 \frac{sin^2(\pi N\left(\frac{D}{\lambda}\right)\left(sin\theta - \tau\left(\frac{c}{D}\right)\right))}{sin^2(\pi\left(\frac{D}{\lambda}\right)(sin\theta - \tau\left(\frac{c}{D}\right)))}$$

Figure 3.13 represents the radiation diagram of a network of eight antennas spaced at a distance $D = \lambda$ for a wavelength λ of 0.03 m and for a

delay $\tau = 4.10^{-11}(s)$. The distribution of the radiated field is shifted from the origin by an angle θ_0 such that $sin\theta_0 = \tau\frac{c}{D}$.

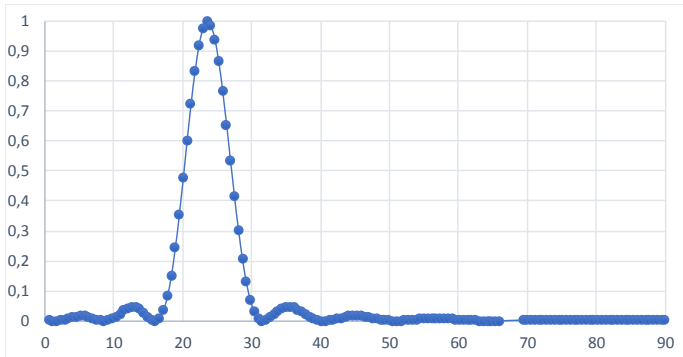

Figure 3.13. *Radiation diagram $E(\theta)^2$ of a network of eight antennas as a function of the angle θ (degrees) in the presence of delays τ such that $\tau\frac{c}{D} = 0,4$ for $D = \lambda = 0.03$ (m). For a color version of this figure, see www.iste.co.uk/dahoo/metrology1.zip*

The introduction of delays does not change the width of the radiated beam and makes it possible to shift the angular position of the central peak of the radiated field. As the origin of the beam emitted by the network shifts by an angle proportional to the delay, it is possible to control the position of the beam by introducing a progressive phase lag gradient on all the antennas in the network and varying the amplitude of this gradient.

3.6.2.3. *Answer to question 3*

If an attenuation a(1-ε) is introduced, the amplitude of the emitted field is proportional to:

$$1 + (1-\varepsilon)\mathrm{a} + (1-\varepsilon)^2\mathrm{a}^2 + \ldots + (1-\varepsilon)^{N-1}\mathrm{a}^{N-1} = \frac{1-(1-\varepsilon)^N\mathrm{a}^N}{1-(1-\varepsilon)\mathrm{a}}$$

For $\varepsilon = 0.05$, the radiated field is attenuated by a factor of 0.84.

Figure 3.14 represents the radiation diagram of a network of eight antennas spaced at a distance $D = \lambda$ for a wavelength λ of 0.03 m, for a delay $\tau = 4.10^{-11}(s)$ and a coefficient $\varepsilon = 0.05$.

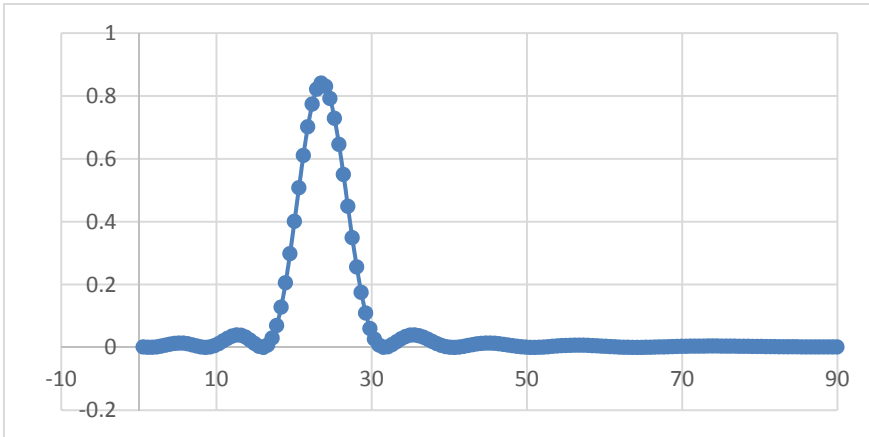

Figure 3.14. *Radiation diagram $E(\theta)^2$ of a network of eight antennas as a function of angle θ (degrees) in the presence of attenuation of 0.05 and delays τ such that $\tau\frac{c}{D} = 0,4$ for $D = \lambda = 0.03 \quad (m)$. For a color version of this figure, see www.iste.co.uk/dahoo/metrology1.zip*

For a network of antennas in which the amplitude and the phase of each elementary antenna can be changed in real time, it is possible to control the direction and the amplitude of the emitted beam. The use of numerical techniques and coding algorithms makes it possible to simultaneously obtain several beams from the same network of antennas (multiple input multiple output or MIMO technology).

4

Smart Materials

Research work in engineering science on applications of a material for its uses in society focuses on its physical and chemical properties that may be of interest. During the Iron Age, the strength of iron based on its mechanical properties, compared to bronze alloys, was a key criterion in the choice of material for the fabrication of weapons and tools. Later on, the scientific methods developed to process materials in laboratories, particularly in materials science, led to the discovery of semiconductors which paved the way to the electronics industry, and hence, the development of electrical systems based on electronics and computer science. Today, the focus of designers is not only in active materials, but also on their uses in microsystems that make them smart, from which the term smart materials is coined. The main characteristic of these materials is the typical coupling of their various physical properties, which recommends their use as active materials. Piezoelectric materials are best known for their uses. The direct effect was discovered by the Curie brothers in 1880, on the Tourmaline crystal, while the converse effect was theoretically predicted by Lippman based on thermodynamic considerations in 1881, and discovered the same year by the Curie brothers.

4.1. Introduction

Materials are the core of any mechanical, electrical, electronic, optical, magnetic, chemical or thermal components and systems. Materials have always been behind the development level of a civilization. Past history reveals that materials were used for dating the evolution in the human way of life starting with the Stone Age (2 million years), the Copper Age and the

Applications and Metrology at Nanometer Scale 1:
Smart Materials, Electromagnetic Waves and Uncertainties,
First Edition. Pierre-Richard Dahoo, Philippe Pougnet and Abdelkhalak El Hami.

Bronze Age (5000 years), and finally the Iron Age (3000 years). A technological breakthrough occurred around 1850, when a low-cost process was developed for steel manufacturing, leading to the construction of railways and modern infrastructures in the industrial world. The resulting metallurgical industry is still active nowadays, because iron or iron-based alloys are needed in the building, construction or transportation sectors.

Empirical methods were replaced by theoretical and analytical ones based on the experience gained by generations of manufacturers and scientists interested in the development of materials. Throughout the Iron Age, new materials were developed, such as ceramics, semiconductors, polymers or composite materials:

– Metals: valence electrons break free from atoms and delocalize in the conduction band; the ions are maintained in the crystal structure, which is generally of a face-centered cubic (fcc), hexagonal compact (hcp) or cubic-centered (cc) type. Metals are characterized by their mechanical strength and ductility. They have good electrical and heat conductivities. If polished, their surface shines.

– Semiconductors: the bonds are covalent. Electrons are shared by the bonded atoms. Electrical conductivity strongly depends on the proportion of impurities or dopants present in the crystal lattice. Examples are Si, Ge and GaAs. The junction diode opened the way for electronics industry.

– Ceramics: the bonds are ionic between positive ions (cations) and negative ions (anions) due to the Coulomb forces. These materials are composed of metallic cations or semiconductor cations in a lattice constituted of oxygen, nitrogen or carbon anions (oxides, nitrides, carbides). They are hard, brittle and insulating. Examples are glass, porcelain and perovskites.

– Polymers: they are bonded by covalent and van der Waals forces, and they are basically formed of carbon C and hydrogen H atoms; however, they may also contain oxygen O and silicon Si atoms. They break down at moderate temperatures (100–400°C), and they are light. Examples are plastics, rubber and silicone gel.

The development of quantum mechanics, starting in the 1930s, made it possible to understand the behavior of materials and the differences in their properties. Atomic interactions could thus be explained, first in atoms, then in molecules and in solids. The combination of physics and chemistry in the

search on the link between the properties of a material and its microstructure is today the field of materials science. This field led to the design of materials and to the knowledge know-how about applications in the field of materials engineering. Industrial processes were developed to manufacture functional devices.

For example, carbon takes various forms: diamond, graphite, nanotubes or fullerenes. The properties of these various forms are related to their underlying structures. The bonds that keep together the atoms in diamond and graphite through shared electrons are covalent.

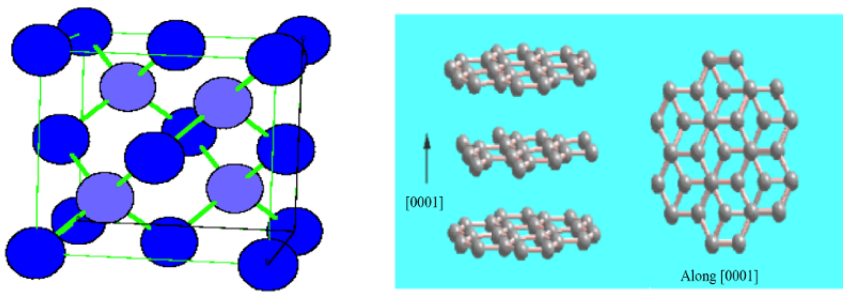

Figure 4.1. *3D diamond structure of fcc type and 2D graphite structure of plane type, two solid-phase forms of carbon. For a color version of this figure, see www.iste.co.uk/dahoo/metrology1.zip*

In the case of diamond, carbon crystallizes in a face-centered cubic structure (Figure 4.1) and uses its four bond possibilities (sp^3 hybridization), which explains its thermal and mechanical stability. All σ bonds are used so that no delocalized electrons are available for electrical conduction, which is the cause of its insulating nature. In the case of graphite (sp^2 hybridization), carbon uses only three electrons for the σ bonds and structured in the form of planes. The π bond (Figure 4.1) is perpendicular to the planes and provides delocalized electrons responsible for its electrical conductivity. As the planes can slide over one another, graphite is ductile.

From a mechanical point of view, diamond is hard and graphite is ductile, and from an electrical point of view, diamond is insulating, while graphite is

conducting. Chapter 9 of [DAH 16] gives an application of carbon nanotubes. Carbon nanotubes can be obtained under high pressure, as indefinitely long wires, which have high mechanical strength.

In order to understand the full complexity of all the naturally occurring materials or synthesized in laboratories, materials are classified into groups. The classification criterion is based on their bonds and not on their structure, properties or uses. There are, however, a few exceptions. For example, for certain materials such as the fiberglass, concrete or wood, the microstructure is a composite of various materials. Biomaterials are any type of biocompatible materials that can replace parts of the human body.

Nowadays, materials science studies the relation between the organization of matter at the nanometric scale and the microstructure and properties of materials. The elaboration of functional materials requires indeed a deep understanding of the relation between structure, properties, fabrication processes and material performance. The materials used in smart systems are characterized by a coupling between various properties. Besides quantum mechanics, the study of material properties involves crystallography, solid-state physics and condensed state matter physics, while the coupling between the properties of the materials is studied in the framework of thermodynamics and statistical physics. Study of the properties of smart materials involves understanding interactions between sub-disciplines in the field of physics and also modeling and simulation.

4.2. Smart systems and materials

A material is qualified as active if under external stimuli it reacts in various ways, according to its nature. When an electric field is applied, its response is a flow of free charges which gives rise to a current if it is a metal or a polarization of matter if it is a dielectric. When a magnetic field is applied, its response is its magnetization if it is a ferromagnetic or ferrimagnetic material. When subjected to a mechanical force, such as the effect of a pressure, it gets more or less deformed if it is a malleable and ductile solid or it breaks if it is rigid. In the case of heat or energy input, its temperature increases either locally, if it is an insulator or throughout its volume and if it is a conductor. Finally, its interaction with an electromagnetic wave leads to absorption, reflection or reflection and

refraction. These characteristics can generally be used in technological systems, and the material is qualified as active.

The term smart material refers to an active material, whose properties are embedded in a system involving a sensor, an actuator and an intelligence supplied by an instrumentation and control system (Figure 4.2), which is able to interact with the environment according to the sensed stimuli and adapt to the external stress. Thus, this system is able to interpret or sense physical or chemical variations in its environment and its effects or consequences. If it has built-in intelligence, it must be able to respond to external stress or excitation by means of an active control mechanism. Such a system has no conscience, but in operation, it presents analogies with a biological system in the living world that is capable of appropriate reaction to the changes in its environment. Hence, such a material is qualified as smart.

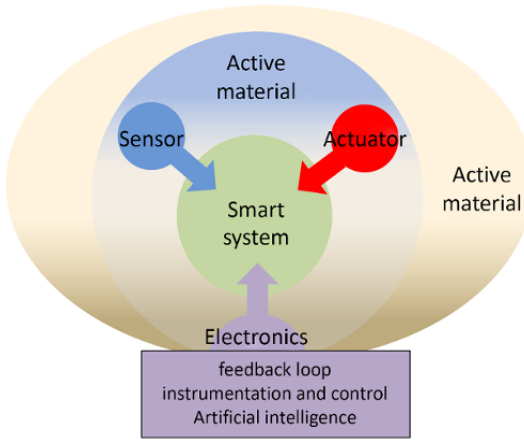

Figure 4.2. *The three elements of a smart system. For a color version of this figure, see www.iste.co.uk/dahoo/metrology1.zip*

However, not all the materials have the functionality that enables them to be integrated in a smart system. The following example illustrates the specific characteristics that a material should have to be qualified as smart material.

Two beams are considered: one made from aluminum (Al) – a metal, and the other one from quartz (SiO_2) – a piezoelectric material. They are both

subjected to a mechanical force. The mechanical and electrical responses to this excitation are then studied. The diagrams of the system setup are shown in Figures 4.3 and 4.4.

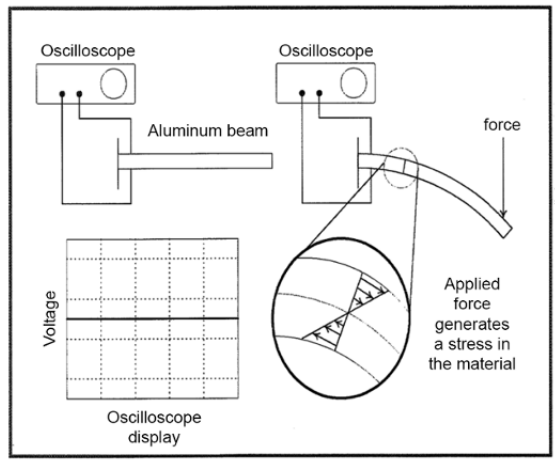

Figure 4.3. *Zero electrical response of an aluminum beam to a mechanical excitation*

In the case of an aluminum beam subjected to a mechanical stress as represented by the bending imposed by a force applied at the end of the beam (Figure 4.3), the oscilloscope displays no electrical response.

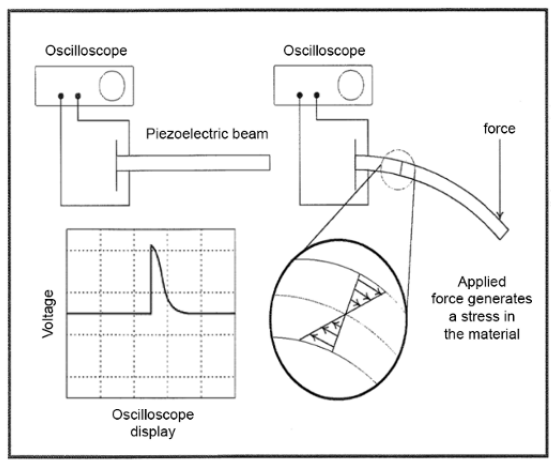

Figure 4.4. *Non-zero response of a piezoelectric beam to mechanical excitation*

In the case of a piezoelectric beam subjected to a mechanical stress as represented by the bending imposed by a force at the end of the beam (Figure 4.4), the oscilloscope displays an electrical response.

The different responses of these two materials – aluminum and piezoelectric material – can be explained, on the one hand, by their structural properties and, on the other hand, by their crystalline symmetry. The structure of aluminum is composed of positive ions or cations linked by a metallic bond to free negative charges, which are peripheral electrons of each aluminum atom, as described in Chapter 5 of [DAH 16]. The applied force induces a mechanical response – namely a bending – as the metal is malleable. Due to the presence of free charges, there is no potential difference at the surface in the absence of an electric field. A piezoelectric material is generally composed of ions that are linked by ionic bonds. Because a mechanical strain is induced by a mechanical force, the material is deformed and as charges are linked by electrostatic forces, the material is polarized. As a result, positive and negative charges are present at the surface. Quartz (SiO_2) is a piezoelectric material. Figure 4.5 shows an example of surface polarization when it is deformed. Because of the mechanical strain, a potential difference can thus be detected – a phenomenon that is observed as an electrical response displayed by an oscilloscope.

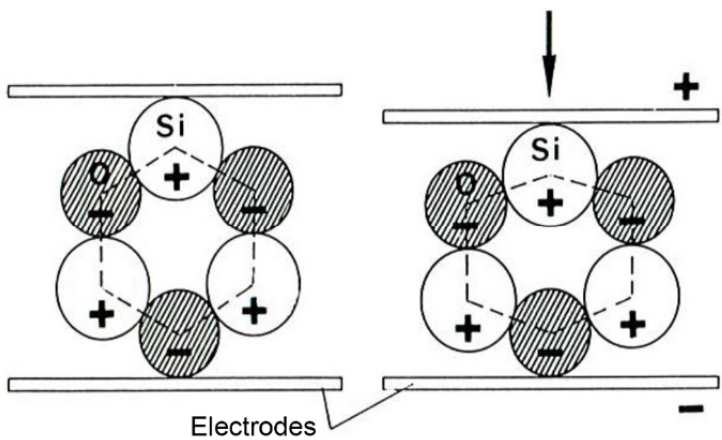

Figure 4.5. *Surface polarization of quartz under mechanical strain*

A metal presents no coupling between its electrical and mechanical properties. In quartz or in a piezoelectric material, there is a coupling between its mechanical and electrical properties. The active materials that are used in smart systems are characterized by the presence of this coupling between two physical or physical and chemical properties of the material. The crystalline structure of the most commonly used piezoelectric crystals is of perovskite type (Figure 4.8) ($CaTiO_3$, $BaTiO_3$, titanates, zirconates, stannates). Piezoelectricity cannot occur in ionic materials, with a high degree of symmetry (this phenomenon requires the absence of a center of symmetry in the unit cell). It is worth noting that the crystalline structure of quartz is hexagonal at high temperature (quartz β) and trigonal at low temperature (quartz α).

The example of quartz shows that for a piezoelectric material, the response is mechanical for an electrical excitation, while an electrical response is obtained for a mechanical excitation. Similar to this electro-mechanical coupling present in quartz, there are other types of couplings, as indicated in Table 4.1: electromagnetic, electro-thermal, electro-optical, thermo-mechanical, pyroelectric, etc. in other materials that can be used as a sensor or an actuator or both.

Following the example of piezoelectric materials, there are (electro-, magneto- or opto-) active polymers, Shape Memory Alloys (SMA), Shape Memory Polymers (SMP), magnetostrictive materials, magneto-rheological fluids, electro-rheological fluids, photochromic materials, polymorphic materials, viscoelastic materials, optical fibers, etc. which are potential candidates to be used as smart materials.

The shape of a piezoelectric or electrostrictive material or of an electroactive polymer changes when voltage is applied. The shape of a shape memory alloy (SMA) changes beyond a certain critical temperature due to a change in structure (phase-transition materials). In magneto-rheological fluids, viscosity changes when a magnetic field is applied. Similarly, the viscosity of electro-rheological fluids changes when an electric field is applied. In a photochromic material, light–matter interaction induces a change in the color of the material. It is worth noting the transition of Micro Electro-Mechanical Systems (MEMS), which contain functional materials towards nanomechanical systems.

Excitation / Response	(Electricity) Current/Charge	(Magnetism) Magnetization	(Mechanics) Strain	(Heat) Temperature	(Optics) Light
(Electricity) Electric field or potential difference	Conductivity Permitivity	Electromagnetic effect	Converse piezoelectric effect Electrostriction Electro-rheological fluid	Electrical resistance Thermoelectric or Peltier effect	Electro-optic Eletcro-chromic Electroluminescent effect
(Magnetism) Magnetic field	Foucault currents	Permeability	Joule effect & Magnetostriction Magneto-rheological fluid	Magnetocaloric effect	Magneto-optic effect
(Mechanics) Stress	Direct piezoelectric effect	Villari effect – reverse magnetostriction	Elasticity modulus Negative Poisson coefficient	Thermomechanical effect	Photoelastic Mechano-chromic effect
(Thermodynamics) Heat	Direct pyroelectric effect Seebeck effect	Thermo-magnetization effect	Thermal expansion and Phase transition	Specific heat	Thermo-luminescence
(Optics) Light	Photovoltaic Photoconductive effect	Photo-magnetization effect	Photostriction	Photo-thermal Thermal Luminescent Thermo-chromic effect	Refraction index Photochromic

Table 4.1. *Smart materials for sensors and actuators*

These materials, which are all characterized by the existence of a coupling between at least two types of properties, have technological applications in many fields, such as electricity and magnetism, electronics, computer science, robotics and mechatronics, technologies related to land and space transportation, and applied science in nanotechnologies (physics, chemistry, biology, etc.). Examples of technological applications are as follows:

– Electrical interconnections, chip carriers, spacer dielectrics, encapsulations, heat dissipaters, heat interface materials, EMI shielding and the casing itself.

– Electric circuit (resistors, capacitors, inductors), electronic devices (diodes, transistors), optoelectronic devices (solar cells, light sensors, electroluminescent diodes) and thermoelectric devices (heaters, coolers, thermocouples).

– Piezoelectric devices (sensors, actuators), micromachines (nanosystems or micro electro-mechanical systems (MEMS)), ferroelectric computer memories, electric interconnections (welding joints, thick film conductors, thin film conductors) and dielectrics (volume, thick film and thin film insulators).

– Substrates for thin films and thick films, heat interface materials in heat dissipaters, cases, electromagnetic interferences (EMI), cables, connectors, electrical supplies, electrical energy storage, motors, electrical contacts (brushes or sliding contacts), etc.

There are various types of actuators as follows: electrostrictive, magnetostrictive, shape memory alloys, viscoelastic materials of magneto-rheological type or electro-rheological type. Sensors can have the form of nanowires in piezoelectric strain gauges or optical fiber strain gauges, constituted of dielectric material structured in the form of digital sensors, in the form of SMA, semiconductor material sensitive to an external physical–chemical stress, in the form of material with giant magneto-impedance (GMI) or giant magneto-resistance (GMR) properties.

There is no single solution for all possible applications. It is sometimes the most appropriate strategy to make an incremental innovation on the existing implementations from initial technologies developed for specific

clients and market needs. It is also possible but risky to implement a technology breakthrough generated by fundamental research laboratories. These breakthrough innovations can be applied in various industrial fields in static heavy structures or mobile light structures.

In the field of civil engineering, examples of heavy structures are buildings, bridges, piers, motorways, airport runways and landfill covers. In the field of civil and military industries, examples of mobile light structures used in land, sea, inland waterway, aeronautics or space transportation are as follows: wheelchairs, electric bicycles, automobiles, trains, ships, trucks, tractors, airplanes, submarines, missiles, satellites, transportable bridges and the constituent elements of these constructions such as vehicle body, bumpers, shaft, windows, engine components, brakes and turbine blades. In everyday life, examples of applications include machinery, sport articles, domestic appliances, computers, connected and electric devices, sport articles such as tennis rackets, fishing rods, skis and many other "manufactured" products. All these industrial products could benefit from the embedded operational intelligence provided by the smart materials.

In the 21st Century, the development of products with increasing levels of functionalities by the use of smart materials will be more and more multisectoral. This will concern the following: transportation, agriculture, food and consumption packaging, construction, sports and leisure, white products and domestic products, healthcare, energy and environment, the Internet of Things, space and defense technologies and in the chemical industry sector opportunities of smart materials development and supply.

The concept of synthetic intelligent and biocompatible materials and devices could replace the inherent failing intelligence functions in our biological systems, as we grow older, for example. Emulating biological mechanisms will provide functionality and intelligence that will allow aging human beings to act in multiple environments. And finally, the development of synthetic smart systems in the form of robots not necessarily of humanoid type in the Living LAB (health care laboratory) could fully replace human functions in certain activities of the common domestic life or of the social and economic life in the industry, in the sector of strenuous work or health damaging tasks.

4.3. Thermodynamics of couplings in active materials

Piezoelectricity is an example of characteristics resulting from couplings between two different physical properties. Probably, the best-known phenomenon is the thermo-mechanical coupling associated with the thermal expansion of a material. It is used as an illustration for the introduction of the notion of couplings in a thermodynamic approach. This is followed by a description of other types of couplings underlying the functionalities described in relation with smart materials. Several applications of piezoelectricity are then presented, including the one already described in the context of technologies applied in near-field microscopy in Chapter 1.

4.3.1. *Thermo-mechanical and thermoelastic coupling*

When a beam is heated at one end, the heat or thermal energy gradually propagates and reaches the other end of the beam. This phenomenon is known as heat conduction. Heat losses should also be considered. These are due to the transfer from the surface of the material to the surroundings, in the form of convection, which is the transfer of thermal energy between a surface and a surrounding fluid (gas or liquid) or in the form of energy transfer by emission of radiation, which is in the infrared domain at ambient temperatures.

A material considered in a first approximation as a homogeneous body expands when its temperature increases. This phenomenon is modeled by a heat expansion coefficient α whose expression is given by:

$$\alpha = -\frac{1}{V}\left(\frac{\partial V}{\partial T}\right)_S \qquad [4.1]$$

where V is the volume of the body, T is the temperature, and S is the state function known as the entropy of the system. In this case, the thermodynamic state of the beam is assumed to move from a state of equilibrium characterized by an initial temperature T and a volume V, to an another state of equilibrium characterized by a temperature $T + dT$ and a volume $V + dV$, without any heat transfer to the external environment, which is known as an adiabatic process (isentropic if the process is reversible).

In the condensed phase, expansion is interpreted at the atomic level at the sub-nanometer scale by the average amplitude of vibration of atoms or ions in their crystallographic sites (anharmonic oscillator model, Chapter 3 of [DAH 16]) which increases when temperature rises. In order to take into account the symmetry properties of the crystallographic systems in which the material crystallizes at the considered temperature, it is more convenient to use tensor calculus [BRI 38, BRU 55, BIO 56, NYE 57, BRU 62, PRI 62, KIT 64, LAN 70] to model this thermo-mechanical effect. It is worth recalling that in a three-dimensional Euclidian space with three Cartesian axes (notation 1 = x, 2 = y and 3 = z) two-by-two orthogonal, the notion of tensor is related to the physical quantity represented by the dyadic product of two vectors. It is in the Riemann space where geodesics are curves, that the notion of tensor fully reveals its significance, particularly in the context of general relativity. Using the tensor notation, the temperature T being a scalar is a zero-order tensor (1 component), the force, which is a vector, is a first-order tensor (3 components) that is denoted by F_k and in order to represent the coupling between two vector quantities considered in the same system of axes, a second-order tensor (9 components) is used, which can be built by the dyadic product of two vectors and third-order tensors, fourth-order tensors, etc., can likewise be defined.

In order to describe the strain of a material, the hypothesis of a continuous medium is generally adopted. At any point of the material, represented by a vector **r**, small displacements represented by a translation vector $\boldsymbol{u}(\boldsymbol{r})$ and the derivatives of the vector with respect to the coordinates are considered. When the material is deformed, at a point represented by $\boldsymbol{r}$, of components x, y, z, each component of $\boldsymbol{u}(\boldsymbol{r})$, $u_x(x, y, z)$, $u_y(x, y, z)$ and $u_z(x, y, z)$ is *a priori* subjected to different modifications along x, y and z. If the material is deformed, the variations of $u_x(x, y, z)$ along x, y and z, namely, the quantities $du_{xx}(x, y, z)= (\partial u_x/\partial x)dx$, $du_{xy}(x, y, z)= (\partial u_y/\partial y)dy$ and $du_{xz}(x, y, z)= (\partial u_z/\partial z)dz$ can be evaluated. Similarly, for the other two components of the vector $\boldsymbol{u}(\boldsymbol{r})$, the various quantities lead to nine possible components for the mathematical representation of this strain.

The case of uniform strain along the three directions, when volume changes without a change in shape, is referred to as hydrostatic compression (or traction). If the shape changes while the volume remains unchanged, this is pure shearing. Nine derivatives are thus obtained, which are represented in

the form of a strain tensor (second-order tensor) which can be split into a symmetric form:

$$\varepsilon_{ik} = \frac{1}{2}\left(\frac{\partial u_i}{\partial x_k} + \frac{\partial u_k}{\partial x_i}\right) \qquad [4.2]$$

and an antisymmetric form:

$$\omega_{ik} = \frac{1}{2}\left(\frac{\partial u_i}{\partial x_k} - \frac{\partial u_k}{\partial x_i}\right) \qquad [4.3]$$

which represent, respectively, the deformation of the material at the point and the rotation of the material about this point.

Figure 4.6 shows a schematic representation of various types of displacements in a material in the context of the study of strains ($\boldsymbol{u}(B_0)$) in a continuous medium that can be split into global translational motion ($\boldsymbol{u}(A_0)$), rotational motion ($\boldsymbol{\omega}(A_0)\wedge d\boldsymbol{r}$) and symmetric strain ($\boldsymbol{\varepsilon}(A_0)d\boldsymbol{r}$) (or vibrations if dynamics is included) where (($u(B_0)$)= ($u(A_0)$) + ($\boldsymbol{\omega}(A_0)\wedge d\boldsymbol{r}$) + ($\boldsymbol{\varepsilon}(A_0)d\boldsymbol{r}$).

In a one-dimensional medium, such as a wire, strain mainly occurs along the axis of the wire. In this case i=1 and k=1, and there is only one term that is ε_{11}, which is denoted by ε. In the case of a plane surface, there are only two possibilities for i and k, so that four terms are to be considered.

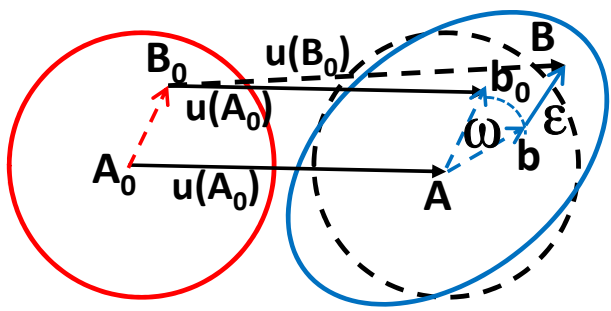

Figure 4.6. *The various displacements of the translational vector u(r) in a material in terms of global translation, rotation and symmetric deformation. For a color version of this figure, see www.iste.co.uk/dahoo/metrology1.zip*

Consider as an exercise the calculation of the strain tensor for a 2D material whose thickness is negligible compared to the other two dimensions, as in the thin film typology discussed in Chapter 1.

The expression of the thermal expansion for a homogeneous variation ΔT of the temperature of the material is:

$$\varepsilon_{ik} = \alpha_{ik} \Delta T \qquad [4.4]$$

where α_{ik} are the coefficients of the symmetric tensor of thermal expansion $[\alpha_{ik}]$ and ε_{ik} are the coefficients of the strain tensor $[\varepsilon_{ik}]$.

This relation can be written in a matrix form as:

$$\begin{pmatrix} \varepsilon_{11} & \varepsilon_{12} & \varepsilon_{13} \\ \varepsilon_{12} & \varepsilon_{22} & \varepsilon_{23} \\ \varepsilon_{13} & \varepsilon_{23} & \varepsilon_{33} \end{pmatrix} = \begin{pmatrix} \alpha_{11} & \alpha_{12} & \alpha_{13} \\ \alpha_{12} & \alpha_{22} & \alpha_{23} \\ \alpha_{13} & \alpha_{23} & \alpha_{33} \end{pmatrix} (\mathrm{T} - \mathrm{T}_0) \qquad [4.5]$$

Given that the strain tensor is symmetric, only six of the nine terms of the tensor are independent. In this case, Voigt (or Voigt-Nye) notation can be used to transform the matrix representation to a vector representation as follows:

$$\begin{pmatrix} \varepsilon_{11} & \varepsilon_{12} & \varepsilon_{13} \\ \varepsilon_{12} & \varepsilon_{22} & \varepsilon_{23} \\ \varepsilon_{13} & \varepsilon_{23} & \varepsilon_{33} \end{pmatrix} \equiv \begin{pmatrix} \varepsilon_{11} \\ \varepsilon_{22} \\ \varepsilon_{33} \\ \varepsilon_{23} \\ \varepsilon_{13} \\ \varepsilon_{12} \end{pmatrix} = \begin{pmatrix} \varepsilon_1 \\ \varepsilon_2 \\ \varepsilon_3 \\ \frac{\varepsilon_4}{2} \\ \frac{\varepsilon_5}{2} \\ \frac{\varepsilon_6}{2} \end{pmatrix} = \begin{pmatrix} \alpha_1 \\ \alpha_2 \\ \alpha_3 \\ \frac{\alpha_4}{2} \\ \frac{\alpha_5}{2} \\ \frac{\alpha_6}{2} \end{pmatrix} (T - T_0) \qquad [4.6]$$

where (ε) and (α) are the vectors with six lines (6x1), and $(T - T_0)$ is a scalar.

On the proper axes of the expansion tensor, the following relation can be written as:

$$\varepsilon_i = \alpha_i \Delta T \qquad [4.7]$$

where α_i is the main expansion coefficients, i=1,2 and 3. In this case, the matrix form is written as:

$$\begin{pmatrix} \varepsilon_1 & 0 & 0 \\ 0 & \varepsilon_2 & 0 \\ 0 & 0 & \varepsilon_3 \end{pmatrix} = \begin{pmatrix} \alpha_1 & 0 & 0 \\ 0 & \alpha_2 & 0 \\ 0 & 0 & \alpha_2 \end{pmatrix} (T - T_0) \quad [4.8]$$

and the vector form as:

$$\begin{pmatrix} \varepsilon_1 \\ \varepsilon_2 \\ \varepsilon_3 \\ 0 \\ 0 \\ 0 \end{pmatrix} = \begin{pmatrix} \alpha_1 \\ \alpha_2 \\ \alpha_3 \\ 0 \\ 0 \\ 0 \end{pmatrix} (T - T_0) \quad [4.9]$$

To model the effects of a mechanical stress in a material according to the formalism of the mechanics of continuous media or the theory of elasticity, elementary volumes are considered for the establishment of the constituent relations. The latter are infinitely small at the macroscopic scale, but very large at the scale of the constituents of the material (atoms, molecules, etc.). During a mechanical deformation of the medium, in the infinitesimal volume around each point, the forces responsible for internal stress are assumed to be short-range and limited to near neighbors. In this case, these forces are exerted by one of its elements on the neighboring elements so that in a given volume inside the material, they can only act at the surface.

The establishment of the constitutive equations requires the definition of the stress tensor acting on an elementary volume of the material. The stress tensor σ_{ik} describes the state of stress at any point of the volume considered in the material and in all the directions. Its components that correspond to a force exerted on a unit surface around a point are homogeneous to a pressure (in Pa or $N.m^{-2}$). It is a symmetric tensor such that $\sigma_{ik} = \sigma_{ki}$. The diagonal terms of the stress tensor are given by tensile (or compression) stresses and non-diagonal terms by shearing stresses. The components have positive values in the case of tension (negative in the case of compression).

In Figure 4.7, the components of the stress tensor are represented by its indices on each face identified by the normal vector n_i.

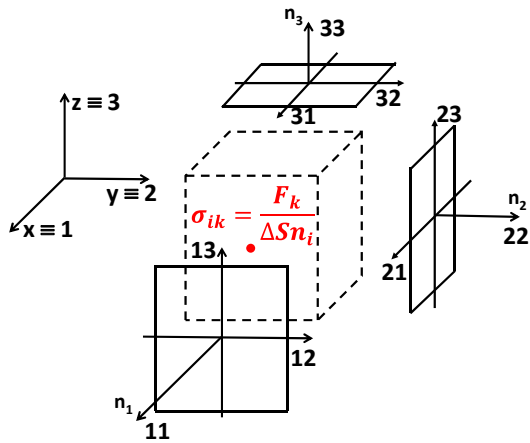

Figure 4.7. *Stress tensor σ_{ik} corresponding to the component k of the force F per unit area acting on the point in the middle of an area defined by its normal n_i. For a color version of this figure, see www.iste.co.uk/dahoo/metrology1.zip*

The matrix form of tensor σ_{ik} is given by:

$$\begin{pmatrix} \sigma_{xx} & \sigma_{xy} & \sigma_{xz} \\ \sigma_{yx} & \sigma_{yy} & \sigma_{yz} \\ \sigma_{zx} & \sigma_{zy} & \sigma_{zz} \end{pmatrix} = \begin{pmatrix} \sigma_{11} & \sigma_{12} & \sigma_{13} \\ \sigma_{12} & \sigma_{22} & \sigma_{23} \\ \sigma_{13} & \sigma_{23} & \sigma_{33} \end{pmatrix} \quad [4.10]$$

Given that the stress tensor is symmetric, similarly to the strain tensor, only six of nine terms of the tensor are independent. Voigt (or Voigt-Nye) notation can be used to transform the matrix representation to the following vector notation:

$$\begin{pmatrix} \sigma_{11} & \sigma_{12} & \sigma_{13} \\ \sigma_{12} & \sigma_{22} & \sigma_{23} \\ \sigma_{13} & \sigma_{23} & \sigma_{33} \end{pmatrix} \equiv \begin{pmatrix} \sigma_{11} \\ \sigma_{22} \\ \sigma_{33} \\ \sigma_{23} \\ \sigma_{13} \\ \sigma_{12} \end{pmatrix} = \begin{pmatrix} \sigma_1 \\ \sigma_2 \\ \sigma_3 \\ \sigma_4 \\ \sigma_5 \\ \sigma_6 \end{pmatrix} \quad [4.11]$$

where (σ) is the vector with six lines (6x1). The first three terms (σ_1, σ_2, σ_3) are the tensile or compression stresses along the perpendicular to surfaces, hence parallel to axes 1, 2 and 3 defined by the normal vector to the surface

and the last three terms ($\sigma_{4,}$,σ_5, σ_6) are the shear stresses about axes 1, 2 and 3 or torques in planes 2-3, 1-3 and 1-2 (Figure 4.7).

The resultant of these forces is given by a volume integral that can be expressed as a surface integral as follows:

$$\iiint_{volume} F_i dV = \iiint_{volume} \frac{\partial \sigma_{ik}}{\partial x_k} dV = \oiint \sigma_{ik} dA_k \qquad [4.12]$$

where F_i is the i^{th} component of the force acting on the volume, $\partial\sigma_{ik}/\partial x_k$ is the divergence of the stress tensor $[\sigma_{ik}]$, dA_k is the elementary surface oriented along the normal defined by the unit vector n_k and where the integral is evaluated on the closed surface surrounding the volume V. Since, by definition, $\sigma_{ik} = \sigma_{ki}$ is the i^{th} component of the force acting on a unit area perpendicular to the axis of x_k (Figure 4.7). Equation [4.10] shows that σ_{ik} dA_k is the i^{th} component of the force acting on the area $d\boldsymbol{A}$.

When a material is subjected to a uniform compression (pressure forces P), known as hydrostatic, then:

$$\sigma_{ik} = -P\delta_{ik} \qquad [4.13]$$

where δ_{ik} is the Kronecker symbol (0 if $i \neq k$, 1 otherwise).

At equilibrium, a strained material verifies (according to the Einstein convention involving summation when indices are repeated) the following relation:

$$\frac{\partial \sigma_{ik}}{\partial x_k} = 0 \qquad [4.14]$$

For small strains, the material returns to its initial unstrained state when external forces are released. In this case, it undergoes elastic strains, and the stored energy density is a state function. On the contrary, if the strain is permanent, the transformation is termed as plastic. It is worth noting that in certain situations, this strain can be viscoplastic.

In the presence of an elastic strain, the variation of internal energy according to the first law of thermodynamics is written as:

$$dU = TdS - \sigma_{ik} d\varepsilon_{ik} \quad [4.15]$$

where the first term corresponds to an exchange in the form of heat, and the second term corresponds to an exchange in the form of mechanical work.

If the applied force is a uniform compression (equation 4.13), the result is the standard expression of the first law of thermodynamics, which reflects the conservation of energy of the system represented by the material such that:

$$dU = TdS - PdV \quad [4.16]$$

The result is, $\delta_{ik} d\varepsilon_{ik}$ being equal to $d\varepsilon_{ii}$, the trace of tensor $[d\varepsilon_{ik}]$. The latter is an invariant that corresponds to the elementary volume dV.

In equation 4.16, T is the intensive variable temperature (an average value over the whole material in equilibrium) and S is the entropy state function, which is an extensive variable (that doubles when volume doubles). Only two of the four laws of thermodynamics are applied, namely, the first law of energy conservation and the second law on the irreversibility of physical processes that stipulates that the entropy of an isolated system always increases. The variation of entropy is defined from the amount of energy exchanged in the form of heat. This variation is zero for a reversible transformation and positive for an irreversible transformation, which is expressed by:

$$dS = \left(\frac{\delta Q}{T}\right)_{rev} + \left(\frac{\delta Q}{T}\right)_{irrev} \quad [4.17]$$

where δQ is the energy supplied as heat. This form of energy modifies neither the external parameters of the system that receives or releases the heat nor the configuration of the system external environment. On the contrary, the energy exchanged in the form of work involves either a modification of the external parameters of the system that receives or releases the work or the configuration of the system external environment or both.

The coupling between two types of properties is the channel through which the energy supplied in one form is transformed in another form. It is appropriate to study the physical phenomena resulting from possible couplings through thermodynamics. The procedure implies identifying the appropriate state function to evaluate this energy transfer from one physical characteristic to another.

Based on equation [4.15], entropy variation can be expressed as:

$$dS = \frac{1}{T} dU + \frac{\sigma_{ik}}{T} d\varepsilon_{ik} \qquad [4.18]$$

A comparison between equations [4.17] and [4.18] reveals the equivalence between the purely thermal form of energy and the mechanical form. Expression [4.15] or [4.18] being convenient for adiabatic processes (S = 0), Helmholtz free energy, $F = U\text{-}TS$ that is obtained from U by the Legendre transform is preferable in the case of isothermal processes (T = 0) as it can be written as:

$$dF = -SdT - \sigma_{ik} d\varepsilon_{ik} \qquad [4.19]$$

Equations [4.15] and [4.19] show that the stress tensor is expressed in the form of a derivative of U at constant entropy or the derivative of F at constant temperature such that:

$$\sigma_{ik} = \left(\frac{\partial U}{\partial \varepsilon_{ik}} \right)_S = \left(\frac{\partial F}{\partial \varepsilon_{ik}} \right)_T \qquad [4.20]$$

The strain tensor can also be expressed as the partial derivative of another potential function. Indeed, choosing by means of another Legendre transform, the thermodynamic potential as $\Phi = F\text{-}\ \sigma_{ik}\varepsilon_{ik}$, it leads to:

$$d\Phi = -\ SdT - \varepsilon_{ik}\, d\sigma_{ik} \qquad [4.21]$$

So that ε_{ik} is determined in the following form:

$$\varepsilon_{ik} = -\left(\frac{\partial \Phi}{\partial \sigma_{ik}} \right)_T \qquad [4.22]$$

Starting from the power series expansion of the Helmholtz free energy, F, or of the internal energy, U, in terms of ε_{ik}, the stress tensor can be expressed as a function of the strain tensor for an isothermal and isentropic strain, respectively, in the following form:

$$\sigma_{ik} = \left(\frac{\partial^2 F}{\partial \varepsilon_{ik} \partial \varepsilon_{lm}} \right)_T \varepsilon_{lm} \text{ or } \sigma_{ik} = \left(\frac{\partial^2 U}{\partial \varepsilon_{ik} \partial \varepsilon_{lm}} \right)_S \varepsilon_{lm} \quad [4.23]$$

These relations are generally expressed in the following form:

$$\sigma_{ik} = C^T_{iklm} \varepsilon_{lm} \text{ or } \sigma_{ik} = C^S_{iklm} \varepsilon_{lm} \quad [4.24]$$

where C_{iklm} are the fourth-order tensors that correspond to isothermal or isentropic stiffness constants. This form corresponds to Hooke's law, which governs linear elasticity.

Likewise, Hooke's law can be expressed in the inverse form:

$$\varepsilon_{ik} = S^T_{iklm} \sigma_{lm} \text{ or } \varepsilon_{ik} = S^S_{iklm} \sigma_{lm} \quad [4.25]$$

where S_{iklm} are compliance constants.

Given that each index can take three values, there are *a priori* $3^4 = 81$ constants. The constants must verify the following symmetry relations: $C_{iklm} = C_{kilm} = C_{ikml} = C_{lmik}$. Indeed, the strain and stress tensors being symmetric ($C_{iklm} = C_{kilm} = C_{ikml}$), there are only 36 possibilities left (the (3+2+1) pairs of indices raised to the power of 2 or 6^2). Furthermore, as the second derivatives verify the Cauchy–Schwarz relation ($C_{iklm} = C_{lmik}$), there are only 21 possibilities (6+5+4+3+2+1) left. It is worth noting that depending on the symmetry elements of a crystal (Appendix and Tables 4.8 and 4.9), this number can be smaller.

The indices of the fourth-order tensor can be contracted, applying the same procedure as for the second-order tensors, ε_{ik} and σ_{ik} using the rule shown in Tables 4.2 and 4.3 for the correspondences between the partitioning (A, B, etc.) of the indices *iklm* of the fourth-order tensor C_{iklm} and those of the indices ik of the second-order tensor C_{ik}.

C_{iklm} lm \ ik	11 22 33	23 31 12	32 13 21
11 22 33	A	B	C
23 31 12	E	F	G
32 13 21	H	I	J

Table 4.2. *Correspondence for contracting indices C_{iklm} to C_{ik}*

C_{ik} k \ i	1 2 3	4 5 6
1 2 3	A	B & C
4 5 6	E & H	F & G & I & J

Tables 4.3. *Correspondence for contracting indices C_{iklm} to C_{ik}*

Relations [4.24] and [4.25] can thus be written as follows:

$$\sigma_i = C_{ik}\varepsilon_k \qquad [4.26]$$

$$\varepsilon_i = S_{ik}\sigma_k \qquad [4.27]$$

where C_{ik} and S_{ik} are 6 x 6 matrices.

The strain and stress tensors being second-order symmetric tensors, they can be decomposed into a spherical part and a deviatory part as follows:

$$\varepsilon_{ik} = (\varepsilon_{ik} - \frac{1}{3}\delta_{ik}\varepsilon_{ll}) + \frac{1}{3}\varepsilon_{ll} \quad [4.28]$$

$$\sigma_{ik} = (\sigma_{ik} - \frac{1}{3}\delta_{ik}\sigma_{ll}) + \frac{1}{3}\sigma_{ll} \quad [4.29]$$

The first term of equation [4.28] corresponds to a sliding or shearing term (strain without change of volume) and the second term to uniform compression (strain without change of shape). The free energy F can then be expressed as follows:

$$F - F_0 = \mu(\varepsilon_{ik} - \frac{1}{3}\delta_{ik}\varepsilon_{ll})^2 + (\lambda + \frac{2}{3}\mu)\varepsilon_{ll}^2 \quad [4.30]$$

$$F - F_0 = \mu(\varepsilon_{ik} - \frac{1}{3}\delta_{ik}\varepsilon_{ll})^2 + \frac{K}{2}\varepsilon_{ll}^2 \quad [4.31]$$

where F_0 is the free energy in the absence of strain, and λ and μ are Lamé coefficients. K is the bulk modulus or rigidity modulus, and μ is the shear modulus ($K > 0$ and $\mu > 0$). These moduli can also be expressed as follows:

$$\mu = \frac{E}{2(1+\nu)} \text{ and } K = \frac{E}{3(1-2\nu)} \quad [4.32]$$

where E is Young's modulus and ν is Poisson's ratio.

The expression of free energy for strains resulting from a variation of temperature is given by:

$$F(T) - F(T_0) = -K\alpha(T - T_0)\varepsilon_{ll} + \mu(\varepsilon_{ik} - \frac{1}{3}\delta_{ik}\varepsilon_{ll})^2 + \frac{K}{2}\varepsilon_{ll}^2 \quad [4.33]$$

where $F(T_0)$ is the free energy in the absence of strain at temperature T_0, and α is the thermal expansion coefficient of the material considered isotropic.

If the nine components of the stress tensor σ_{ik} and the temperature T are considered as independent variables, the variations of the strain tensor components ε_{ik} and of the entropy state function S can be expressed as a function of these independent variables, σ_{ik} and T. Similarly, the components of the strain tensor ε_{ik} and the entropy state function S can be taken as independent variables and the variations of the components of the stress tensor σ_{ik} and of temperature T can be expressed as a function of ε_{ik} and S.

The following equations are obtained with the first set of variables:

$$d\varepsilon_{ik} = \left(\frac{\partial \varepsilon_{ik}}{\partial \sigma_{lm}}\right)_T d\sigma_{lm} + \left(\frac{\partial \varepsilon_{ik}}{\partial T}\right)_\sigma dT \qquad [4.34]$$

$$dS = \left(\frac{\partial S}{\partial \sigma_{lm}}\right)_T d\sigma_{lm} + \left(\frac{\partial S}{\partial T}\right)_\sigma dT \qquad [4.35]$$

The physical significance of these four partial derivatives can be easily established with the following approach, by considering the variations of ε_{ik} and S, when dT=0 (isothermal) and $d\sigma_{lm}$ =0 (constant stress). The first term of [4.34] corresponds to the isothermal elastic coefficients as already obtained with the free energy function F and denoted: $\left(\frac{\partial \varepsilon_{ik}}{\partial \sigma_{lm}}\right)_T = S^T_{iklm}$ (equation [4.25]). The superscript designates the parameter that is constant. The second term represents the thermal expansion coefficients: $\alpha_{ik} = \left(\frac{\partial \varepsilon_{ik}}{\partial T}\right)_\sigma$ (equation [4.44]). The first term of equation [4.35] corresponds to the entropy increase following stresses in an isothermal process. This term corresponds to the ratio of the heat generated as result of these stresses and the temperature T, hence $\left(\frac{\partial S}{\partial \sigma_{lm}}\right)_T = \frac{\delta Q}{T}$, which is the piezo-caloric effect. If the second term of equation [4.35] is multiplied by T, hence $T\left(\frac{\partial S}{\partial T}\right)_\sigma = C^\sigma$, the result corresponds to the heat released when the stress is maintained constant (equivalent to a constant pressure) which corresponds to the heat capacity C^σ per unit volume under constant stress. Given the interactions between the effects related to these coefficients, the latter are not independent.

Based on the potential Φ, and on the variation $d\Phi$ (equation [4.21]), the following relation can be written as:

$$\frac{\partial^2 \Phi}{\partial \sigma_{lm} \partial T} = -\left(\frac{\partial S}{\partial \sigma_{lm}}\right)_T = -\left(\frac{\partial \varepsilon_{lm}}{\partial T}\right)_\sigma \quad [4.36]$$

which shows that there is a relation between the thermal expansion coefficient and the piezo-caloric coefficient. For small variations, the integration of equations [4.34] and [4.35] leads to the following equations:

$$\varepsilon_{ik} = S^T_{iklm}\sigma_{lm} + \alpha_{ik}\Delta T \quad [4.37]$$

$$\Delta S = \alpha_{ik}\sigma_{ik} + \frac{C^\sigma}{T}\Delta T \quad [4.38]$$

After contraction of the indices, these equations between tensors are simplified and can be written as:

$$\varepsilon_i = S^T_{ik}\sigma_k + \alpha_i \Delta T \quad [4.39]$$

$$\Delta S = \alpha_i \sigma_i + \frac{C^\sigma}{T}\Delta T \quad [4.40]$$

These equations can be written in the form of matrix equations as:

$$\varepsilon = S^T \sigma + \alpha \Delta T \quad [4.41]$$

$$\Delta S = \alpha \sigma + \frac{C^\sigma}{T}\Delta T \quad [4.42]$$

It is worth noting that in the presence of a heat flux, the heated region cannot freely expand and that it is subjected to compression stresses of the colder regions. Similarly, the colder regions are subjected to tensile stresses exerted by the warmer regions. In this case, these additional stresses must be taken into account when applying Hooke's law.

It can thus be shown that

$$\sigma_{ik} = -3K\alpha(T - T_0) + 2\mu\varepsilon_{ik} + \frac{E\nu}{(1+\nu)(1-2\nu)}\varepsilon_{ll}\delta_{ik} \quad [4.43]$$

and

$$\varepsilon_{ik} = \alpha(T - T_0)\delta_{ik} + \frac{1+\nu}{E}\sigma_{ik} - \frac{\nu}{E}\sigma_{ll}\delta_{ik} \quad [4.44]$$

These equations are applied to determine the strain when temperature varies. In the weak coupling mode, the thermal effect is first evaluated, and from the new set of values of the different parameters, the mechanical effect is then evaluated and so on in a feedback loop until the final thermodynamic state is reached. In the strong coupling mode, both effects must be considered simultaneously.

4.3.2. *Multiphysics couplings*

The connection between the electric and magnetic phenomena was established in the 19th Century, when Oersted discovered that an electric current generates a magnetic field. This effect was observed by the deviation of a compass needle when an electric current starts or stops flowing through a conductor during a Joule effect didactic experiment. A thermoelectric effect leads to a temperature increase, when an electric current flows through a metallic material. The electromagnetic properties of matter are described in terms of electric polarization and magnetization, locally defined as densities of dipolar electric moments and dipolar magnetic moments in the context of Maxwell's equations by assuming that the material that is polarized when subjected to an electric or magnetic field is in the form of a continuous medium. Table 4.4 summarizes the fundamental relations of electromagnetism.

Medium	Isotropic	Anisotropic	Constant
Dielectric	$\mathbf{D}=\varepsilon\mathbf{E}$ $\mathbf{P}=\varepsilon_0\chi_e\mathbf{E}$ $\mathrm{div}\varepsilon_0\mathbf{E}=-\mathrm{div}\mathbf{P}$	$\mathbf{D}=\varepsilon\mathbf{E}$ $\mathbf{P}=\varepsilon_0\chi_e\mathbf{E}$ $\mathrm{div}\varepsilon_0\mathbf{E}=-\mathrm{div}\mathbf{P}$	Permittivity Electric susceptibility
Magnetic	$\mathbf{B}=\mu\mathbf{H}$ $\mathbf{J}=\mu_0\chi_m\mathbf{H}$ $\mathrm{rot}\mu_0\mathbf{H}=\mathrm{rot}\mathbf{J}$	$\mathbf{B}=\mu\mathbf{H}$ $\mathbf{J}=\mu_0\chi_m\mathbf{H}$ $\mathrm{rot}\mu_0\mathbf{H}=\mathrm{rot}\mathbf{J}$	Permeability Magnetic susceptibility
Conductor	$\mathbf{E}=\rho_e\mathbf{j}$ $\mathbf{j}=\sigma_e\mathbf{E}$	$\mathbf{E}=\rho_e\mathbf{j}$ $\mathbf{J}=\sigma_e\mathbf{E}$	Resistivity Electrical conductivity
Superconductor	$\mathrm{d}\mathbf{j}/\mathrm{d}t=(1/\mu_0\lambda^2_s)\mathbf{E}$ $\mathbf{j}=-(1/\mu_0\lambda^2_s)\mathbf{A}$		Skin depth

Table 4.4. *Fundamental laws for linear electromagnetic media*

Most of the discoveries concerning functional materials characterized by a coupling between two types of properties can also be traced back to the 19th Century. The origin and the comprehension of the coupling between various physical properties within the same material is still an active research subject in condensed matter physics. The existence of materials with couplings that involve several properties simultaneously has been demonstrated. In the ferroics, for example, the coupling depends on the shaping of the material, on the crystallographic structure and on the configuration of the magnetic spins. These materials are characterized by properties such as ferromagnetism, ferroelectricity and/or ferroelasticity.

A thermoelectric effect of another kind was revealed by Thomas Johann Seebeck in 1821. He discovered that a metallic needle is deviated when it is placed between two conductors of different kinds connected by junctions at their ends and subjected to a thermal gradient (Seebeck effect). The observed effect has an electric origin, although Seebeck first associated the cause with a magnetic field. An electric potential difference appears at the junction between the two different materials subjected to a temperature difference. The most widely known application of the Seebeck effect is the measurement of temperature using thermocouples. The pyroelectric effect studied by Antoine Becquerel in 1828 is another thermo-electric effect. The direct effect is the appearance of polarization or charges under thermal excitation, while the inverse effect is the electro-caloric effect, with the emission of heat or a warming effect under electric excitation. An example of such a material is lithium tetra-borate ($Li_2B_4O_7$) in which a change in temperature leads to a variation of the electric polarization of the crystal. Finally, in 1834, Jean-Charles Peltier discovered another thermoelectric effect: a temperature difference appears at the junction between two different materials subjected to an electric current (see the Peltier effect). Between 1878 and 1893, Lord Kelvin developed the theory leading to the interpretation of the properties of pyroelectric materials and of the Seebeck and the Peltier effects. In a material subjected to a temperature gradient and through which an electric current flows, heat exchanges occur with the external environment. Conversely, an electric current is generated by a material through which there is a heat flux. The Thomson effect, the Seebeck effect and the Peltier effect show similarities. However, the Thomson effect is different from the other ones because only one conductive material is necessary for its occurrence.

Magnetostriction was discovered in 1842 by the English physicist Joule when an iron beam was placed in a magnetic field. Electrostriction was predicted and verified by Jacques and Pierre Curie in 1881 on a quartz crystal. It is an electromechanical effect that depends on the squared of the intensity of the electric field inducing the material strain. This is known as an electrostriction effect and is generally negligible.

The piezoelectric effect is another electromechanical effect that was experimentally discovered in the tourmaline crystal (hemihedral crystals with inclined faces) by the Curie brothers, Jacques and Pierre, in 1880 [CUR 80]. Combining their knowledge on pyroelectricity and on the crystalline structure, they predicted and verified the existence of piezoelectricity in materials such as quartz, tourmaline, topaz, sugar and Rochelle salt crystals, which become polarized under the effect of a pressure. The possibility of the reverse effect was predicted the following year by Gabriel Lippmann [LIP 81, LIP 81b] as a result of thermodynamic calculations and was verified the same year by the Curie brothers [CUR 81]. In the same year 1881, Wilhelm Hankel used the term piezoelectricity originating in the Greek word “piezein”, meaning to press or push, to qualify this phenomenon. In 1910, the theory of this effect was described in the context of tensor formalism and crystallography by Woldemar Voigt [VOI 10, VOI 28]. He listed the 20 crystalline classes (absence of a center of symmetry) that can present piezoelectricity and specified the piezoelectric constants according to the crystalline structures. In a first approximation piezoelectricity is a linear effect as the strain is proportional to the applied electric field. The electromechanical coupling coefficient, which is the essential parameter for the description of piezoelectric materials, reflects the conversion of electric energy into mechanical energy and vice versa.

Piezoelectric materials are available in various forms:

− Monocrystals: this is the form of the piezoelectric materials found in nature, such as the insulating dielectrics quartz or tourmaline, the semiconductors CdS or AsGa, the oxide ZnO or the ferroelectric monocrystal LiNbO.

− Ferroelectric ceramics ($BaTiO_3$ or $Pb(Zr, Ti)O_3$), based on a material with perovskite structure (Figure 4.8), which are the most widely used, mainly due to their ease of fabrication and the many properties conferred by the perovskite structure when the chemical composition and the manufacturing parameters are varied.

– Composites, whose electromechanical coupling coefficient is higher than that of conventional ceramics.

– Polymers (polyvinylidene fluoride PVDF, polyvinyl chloride PVC)), whose ease of fabrication allows a variety of elaboration process and have the advantage of being very flexible. Their coupling coefficients are nevertheless quite low.

– Biological materials, such as cellulose, amylose, keratin, polypeptides and polyaminoacids.

Perovskite is a natural mineral with the chemical formula $CaTiO_3$. It is the prototype of many materials whose structure is of the type ABO_3 (Figure 4.8). This structure is very stable and enables the manufacturing of a very large number of components with a wide variety of properties that can be used in many practical applications. The key role of the BO_6 octahedrons is to confer to the crystal the property of being ferromagnetic or/and ferroelectric. These materials are formed of oxygen octahedrons linked by their vertices their centers being the sites where cations B are located. Cations A, of larger size, are located in the cuboctahedric cavity formed by eight octahedrons. In this ideal structure, a factor t or a Goldsmith factor can be defined in relation to the radii of various ions. When it is equal to 1, the prototype structure is stable.

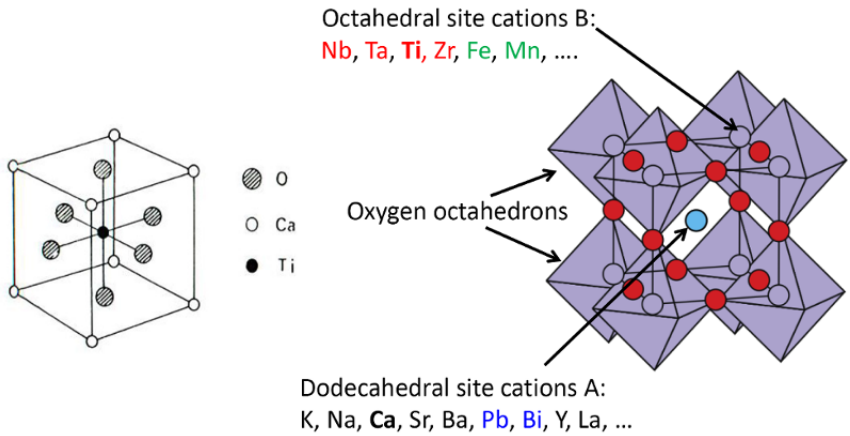

Figure 4.8. *Octahedral and dodecahedral sites of $CaTiO_3$ perovskite with ABO_3 structure. For a color version of this figure, see www.iste.co.uk/dahoo/metrology1.zip*

The crystals whose unit cell has no center of symmetry (non-centrosymmetric) have all piezoelectric properties with the exception of crystals described by 432 point symmetry. Piezoelectric crystals can be classified into 20 point groups (32 groups – 11 centrosymmetric – 1). However, the appearance of piezoelectricity requires the application of an electric or mechanical external stress in a given direction, as the effect is not isotropic.

The direct piezoelectric effect can be described by means of a third rank tensor denoted by d_{ikl}, which links polarization to mechanical stress σ_{kl} such as:

$$D_i = d_{ikl}\sigma_{kl} \qquad [4.45]$$

The stress tensor being symmetric, the number of independent coefficients is reduced from 27 (3^3) to 18 (3x3x2 or 3x6, or 3 possibilities for i and 6 for kl). If the crystal has symmetry elements, this number is lowered and reduces to 4 in quartz and to 3 in barium titanate ($BaTiO_3$).

Indices of third-order tensor can also be contracted by considering the symmetry properties according to the Voigt convention shown in Table 4.5.

d_{ikl}	i11	i22	i33	i23 i32	i31 i13	i12 i21
d_{ik}	i1	i2	i3	i4	i5	i6

Table 4.5. *Correspondence for contracting the indices from d_{ikl} to d_{ik}*

A relation in the following matrix form is obtained as:

$$D_i = d_{ik}\sigma_k \qquad [4.46]$$

The converse piezoelectric effect can be described using a third rank tensor that is also denoted by d_{ikl} which links the strain to the electric field E_k:

$$\varepsilon_{ik} = d_{ikl}E_k \qquad [4.47]$$

The contraction of indices leads to a matrix relation that can be written in the following form:

$$\varepsilon_i = d_{ik}E_k \qquad [4.48]$$

It can be shown [NYE 57] that the piezoelectric coefficients of the direct and converse effect are equal provided that the following correspondences are used during the contraction of indices:

$$\begin{pmatrix}\sigma_{11} & \sigma_{12} & \sigma_{13}\\ \sigma_{21} & \sigma_{22} & \sigma_{23}\\ \sigma_{31} & \sigma_{32} & \sigma_{33}\end{pmatrix} = \begin{pmatrix}\sigma_1 & \sigma_6 & \sigma_5\\ \sigma_6 & \sigma_2 & \sigma_4\\ \sigma_5 & \sigma_4 & \sigma_3\end{pmatrix} \equiv \begin{pmatrix}\sigma_1\\ \sigma_2\\ \sigma_3\\ \sigma_4\\ \sigma_5\\ \sigma_6\end{pmatrix} \qquad [4.49]$$

$$\begin{pmatrix}\varepsilon_{11} & \varepsilon_{12} & \varepsilon_{13}\\ \varepsilon_{21} & \varepsilon_{22} & \varepsilon_{23}\\ \varepsilon_{31} & \varepsilon_{32} & \varepsilon_{33}\end{pmatrix} = \begin{pmatrix}\varepsilon_1 & \frac{1}{2}\varepsilon_6 & \frac{1}{2}\varepsilon_5\\ \frac{1}{2}\varepsilon_6 & \varepsilon_2 & \frac{1}{2}\varepsilon_4\\ \frac{1}{2}\varepsilon_5 & \frac{1}{2}\varepsilon_4 & \varepsilon_3\end{pmatrix} \equiv \begin{pmatrix}\varepsilon_1\\ \varepsilon_2\\ \varepsilon_3\\ \frac{1}{2}\varepsilon_4\\ \frac{1}{2}\varepsilon_5\\ \frac{1}{2}\varepsilon_6\end{pmatrix} \qquad [4.50]$$

with

$$\begin{pmatrix}d_{11} & d_{12} & d_{13} & d_{14} & d_{15} & d_{16}\\ d_{21} & d_{22} & d_{23} & d_{24} & d_{25} & d_{26}\\ d_{31} & d_{32} & d_{33} & d_{34} & d_{35} & d_{36}\end{pmatrix} = \begin{pmatrix}d_{111} & d_{122} & d_{133} & \frac{d_{123}}{2} & \frac{d_{131}}{2} & \frac{d_{112}}{2}\\ d_{211} & d_{222} & d_{233} & \frac{d_{223}}{2} & \frac{d_{231}}{2} & \frac{d_{212}}{2}\\ d_{311} & d_{322} & d_{333} & \frac{d_{323}}{2} & \frac{d_{331}}{2} & \frac{d_{312}}{2}\end{pmatrix} \qquad [4.51]$$

Table 4.6 summarizes the equations defining the direct and converse piezoelectric effects.

	Tensor notation	Matrix notation
Direct effect	$D_i=d_{ikl}\sigma_{kl}$	$Di=dik\sigma k$
Converse effect	$\varepsilon_{ik}=d_{lik}E_l$	$\varepsilon_i=d_{li}E_l$

Table 4.6. *Piezoelectric effect in tensor and matrix notation*

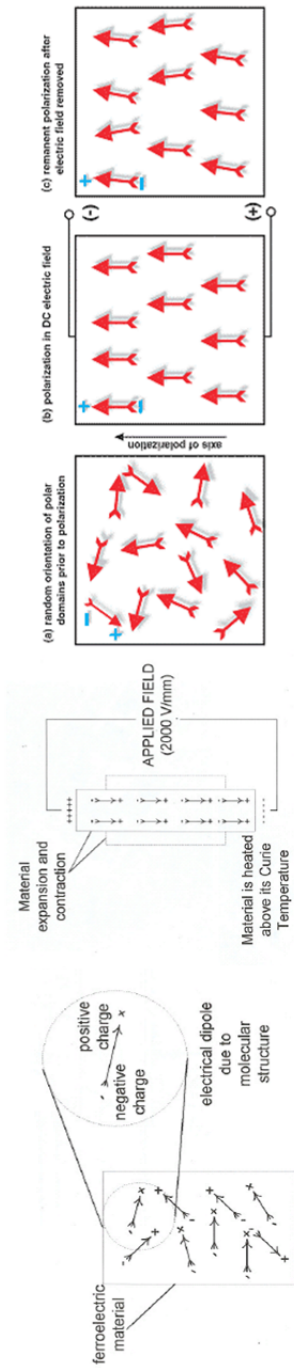

Figure 4.9. *Poling of a ferroelectric material. For a color version of this figure, see www.iste.co.uk/dahoo/metrology1.zip*

The family of piezoelectric ceramics forms an important group of materials. There are polycrystalline ferroelectric materials, most of which have a tetragonal/rhombohedral structure, close to the cubic structure. There are also mixtures of lead oxide, the most common of which is PZT. Unlike quartz, for example, these materials must be polarized in order to exhibit a piezoelectric effect. On the contrary, the latter is much stronger. Typically, a PZT beam subjected to an electric field presents a strain that is several hundred times greater than that of a quartz beam of similar size subjected to the same field.

The process used for the fabrication of piezoelectric materials is known as poling. The procedure for poling a ferroelectric material involves the alignment of electric dipoles that are randomly oriented in the material in the direction of an electric field when it is maintained at a temperature above its transition temperature. During the alignment, the material undergoes an elongation along the direction of the electric field and a contraction of its lateral dimensions. Then while maintaining the electric field the temperature is lowered (field cool). The material thus maintains a residual macroscopic polarization, the dipoles being nearly aligned even below the transition temperature after the removal of the electric field. The process is schematically represented in Figure 4.9.

As mentioned in the previous section for the thermo-mechanical effect and the piezo-caloric coupling, a system at equilibrium can be fully characterized if the extensive and intensive variables that determine the state functions are known, relying on the laws of thermodynamics. For piezoelectric materials, the quantities used are the entropy, the strain and the polarization of the material system, which are variables of a thermodynamic potential. Gibbs free energy is generally used, which is a function of intensive quantities: temperature, electric field and stress. It is expressed as:

$$\Phi = U - \sigma_{kl}\varepsilon_{kl} - E_k D_k - TS \qquad [4.52]$$

hence:

$$\mathrm{d}\Phi = -\varepsilon_{kl} d\sigma_{kl} - D_k dE_k - SdT \qquad [4.53]$$

with

$$-\left(\frac{\partial^2\Phi}{\partial\sigma_{kl}\partial E_i}\right)_T = \left(\frac{\partial\varepsilon_{kl}}{\partial E_i}\right)_{\sigma,T} = -\left(\frac{\partial D_i}{\partial\sigma_{kl}}\right)_{E,T} = d_{ikl}^T \quad [4.54]$$

$$-\left(\frac{\partial^2\Phi}{\partial\sigma_{kl}\partial T}\right)_E = \left(\frac{\partial\varepsilon_{kl}}{\partial T}\right)_{\sigma,E} = -\left(\frac{\partial S}{\partial\sigma_{kl}}\right)_{E,T} = \alpha_{kl}^E \quad [4.55]$$

$$-\left(\frac{\partial^2\Phi}{\partial E_i\partial T}\right)_\sigma = \left(\frac{\partial S}{\partial E_i}\right)_{\sigma,T} = -\left(\frac{\partial D_i}{\partial T}\right)_{\sigma,E} = p_i^\sigma \quad [4.56]$$

These relations obtained from the second derivatives of the thermodynamic potential show that the direct and converse piezoelectric coefficients are equal (equation [4.54]). The same is applicable to thermal expansion coefficients and piezo-caloric coefficients (equation [4.55]) and also to pyroelectric coefficients and to electro-caloric coefficients (equation [4.56]).

The following relations can thus be determined:

$$\varepsilon_{ik} = S_{iklm}^{E,T}\sigma_{lm} + d_{lik}^T E_l + \alpha_{ik}^E \Delta T \quad [4.57]$$

$$D_i = d_{ikl}^T\sigma_{kl} + \chi_{ik}^{\sigma,T}E_k + p_i^\sigma \Delta T \quad [4.58]$$

$$\Delta S = \alpha_{ik}^E\sigma_{ik} + p_i^\sigma E_i + \frac{C^{\sigma,E}}{T}\Delta T \quad [4.59]$$

The transformation from the tensor notation to the matrix notation can be done by contracting the indices and writing the constitutive equations in the following form:

$$\varepsilon = S^{E,T}\sigma + d^T E + \alpha^E \Delta T \quad [4.60]$$

$$D = d^T\sigma + \chi^{\sigma,T}E + p^\sigma \Delta T \quad [4.61]$$

$$\Delta S = \alpha^E\sigma + p^\sigma E + \frac{C^{\sigma,E}}{T}\Delta T \quad [4.62]$$

If the temperature is assumed to be constant, the constitutive equations for the study of piezoelectric phenomena are written as follows:

$$\varepsilon = S^E\sigma + dE \quad [4.63]$$

$$D = d\sigma + \chi^\sigma E \quad [4.64]$$

$$\Delta S = \alpha^E\sigma + p^\sigma E \quad [4.65]$$

The constitutive equations for the couplings involving the magnetic field or other types of stresses can be established from potential functions obtained by the Legendre transform from the internal energy U in order to recover the relevant independent variables.

A magnetostrictive material changes its shape (crystalline structure) when it is exposed to a magnetic field. Magnetostrictive expansion can be used to create a linear motion with strong forces and very short response times. Magnetostrictive actuators are efficient, operate at low voltage, transmit large amounts of energy per volume and enable contactless action (distant magnetic field). The material can be deposited in thin films for the manufacturing of microsystems or nanosystems. An example of material is based on Terfenol, an alloy of Terbium, Dysprosium and iron ($Tb_{0,3}Dy_{0,7}Fe_{1,9}S$). It is a magnetostrictive material that makes it possible to gain an order of magnitude on the common piezoelectric components (known as giant magnetostriction). Another magnetostrictive material is Permendur (alloy composed of 49% Fe, 49% Co and 2% V).

Shape memory alloys (SMA) present phase transition phenomena, the alloy transforming from a given structure to another. The material changes its length as a function of temperature following a thermo-mechanical coupling. One of the most common alloys is a combination of nickel and titanium. This shape memory alloy can be processed so that it contracts when it reaches a defined temperature. When it cools, it returns to its original shape. This technology can be used to open a valve in a coffee machine at a defined temperature. When embedded in a deformable material in the form of wires, such materials enable a response depending on a current flow. The material retracts and can be used in robotics technology for feel-touch operation. Figure 4.10 shows the different steps in the development of such a material.

The metallurgical phases involved in the process are the martensite phase at low temperature and the austenite phase at high temperature. When there is a phase transformation, the SMA modifies its shape, hence it undergoes a two-way shape "memory" effect. The SMA process starts with the material annealed at high temperature in the austenite phase (Figure 4.10). The shape is in this way fixed in the material. During cooling, the material transforms into the martensite phase and adopts an interlaced crystalline structure. When subjected to a mechanical strain, the interlaced crystalline structure transforms to an asymmetric crystalline structure.

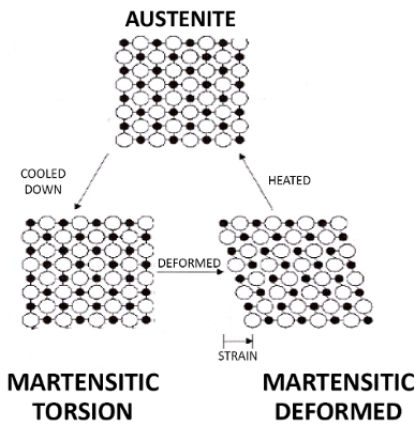

Figure 4.10. *Shape memory alloy development process*

During heating, the martensite phase transforms into austenite and the shape initially imposed by annealing is recovered. In this way, the permanent deformation created by the onset of the martensite phase is suppressed and the material returns to its initial state memorized during the annealing at austenitic temperatures. If the recovery is mechanically prevented, stresses up to 700 MPa can be developed.

Table 4.7 summarizes several orders of magnitude for several active materials that can be included in smart systems.

	Shape Memory Alloy	Piezoelectric	Giant magnetostrictive	Bimorph actuators
Physical phenomenon	Martensitic transformation	Piezoelectricity	Magnetostriction	Differential thermal expansion
External physical stress	Thermal	Electric field	Magnetic field	Thermal
Energy density (J/m^3)	10^6 to 10^7	10^2 (PZT) 10^3 (PMN)	10^6 to 10^7 (Terfenol D)	10^6 (Ni/Si)
Bandwidth	Low	High	High	Low
Working mode	Bending, torsion, tension, compression	Depends on the direction of the electric field	Depends on the direction of the magnetic field	Bending
Typical strain	**1% to 8%	0.12% to 0.15%	0.58% to 0.81%	5% to $23x10^{-4}$
	*Strongly dependent on shape and size **Depends on lifetime specification (Maximal strain up to 15% of a monocrystal)			*Strongly dependent on shape and size

Table 4.7. *Orders of magnitude of the characteristics of some active materials*

4.4. Exercises on the application of active materials

4.4.1. *Strain tensor for 2D thin films*

In this exercise, the elements of a strain tensor are calculated for a plate or thin film, whose thickness is negligible compared to its lateral dimensions. The results can be applied to the calculation of the strain of a substrate subjected to a given temperature during thin film deposition, for example.

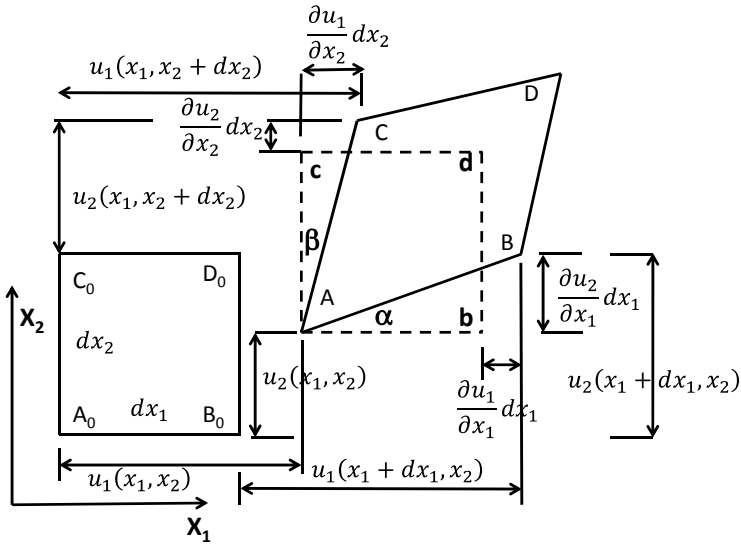

Figure 4.11. *Displacement vectors to calculate the strain tensor in 2D*

4.4.1.1. *Questions*

1) Recall the principle of the model used for the calculation of the strain tensor using Figure 4.11 as a reference.

2) Provide an interpretation of the square in Figure 4.11 in the model used for the calculation of the strain tensor using Figure 4.6 as a reference.

3) Provide an interpretation of the rhomboid in Figure 4.11 in the model used for the calculation of the strain tensor using Figure 4.6 as a reference.